Superconductivity and magnetism in heavy-fermion UPd2(Al,Ga)3

Suellow, S.; Ludolph, B.; Becker, B.; Nieuwenhuys, G.J.; Menovsky, A.A.; Mydosh, J.A.

Published in:
Physical Review. B, Condensed Matter

DOI:
10.1103/PhysRevB.56.846

Superconductivity and magnetism in heavy-fermion $UPd_2(Al,Ga)_3$

S. Süllow, B. Ludoph, B. Becker, G. J. Nieuwenhuys, A. A. Menovsky, and J. A. Mydosh
Kamerlingh Onnes Laboratory, Leiden University, 2300 RA Leiden, The Netherlands
(Received 8 October 1996)

We present bulk properties (resistivity, specific heat, and susceptibility) of the quasiternary system $UPd_2(Al_{1-x}Ga_x)_3$ and derive the superconducting and magnetic phase diagrams. For low Ga substitution ($x \leqslant 0.25$) a complete suppression of superconductivity is found, while the magnetic properties are hardly affected. For larger x the magnetic transition temperature T_N gradually decreases, and the mass enhancement of the electrons increases, until at $x=0.8$–0.9 a crystallographic transition takes place from the $PrNi_2Al_3$ to the BaB_2Pt_3 lattice. At the structural transition T_N discontinuously increases, while the electronic specific heat γ grows smoothly through the transition. We discuss the relationship between the alloying parameter x and the magnetic ordering and electronic hybridization, respectively. The strong suppression of the superconductivity in UPd_2Al_3 with Ga suggests an unconventional mechanism of superconductivity, most probably related to spin fluctuations mediating the pairing. [S0163-1829(97)01126-0]

I. INTRODUCTION

Hexagonal 123 compounds UT_2M_3, T=Ni and Pd and M=Al or Ga, were the subject of many detailed investigations in recent years for two main reasons:[1–3] The first is the appearance of heavy-fermion superconductivity in UNi_2Al_3 (Ref. 1) and UPd_2Al_3 (Ref. 2) (both crystallizing in the $PrNi_2Al_3$ lattice), and the second relates to the competition between the Kondo effect and magnetic interaction.

Heavy-fermion superconductivity is a topic of major interest in current research, since the superconductivity is carried by strongly correlated electrons which also mediate and transmit the magnetic interactions (for a review see Ref. 4). Here the pairing mechanism of the superconductivity might be different from that of the conventional phonon-coupled BCS superconductors; for instance, magnetic correlations or spin fluctuations could be involved.

Recently, we presented the basic properties of UPd_2Ga_3,[3] an allomorph to UPd_2Al_3. This system crystallizes in the BaB_2Pt_3 structure, which is a superstructure of the $PrNi_2Al_3$ lattice. Its general properties qualitatively resemble those of UPd_2Al_3. Quantitatively, the electronic specific heat γ is larger, while the magnetically ordered moment μ_{ord}, transition temperature T_N, and the crystalline electric field (CEF) splitting of the low-lying levels are all smaller. Nevertheless, UPd_2Ga_3 was not found to be superconducting down to 50 mK. Hence, the replacement of Al in UPd_2Al_3 by Ga mainly affects the superconducting behavior, while the magnetism is hardly influenced. In order to investigate the dependence of $UPd_2(Al,Ga)_3$ on the local site symmetry of the uranium, alloying experiments using $UPd_2(Al_{1-x}Ga_x)_3$ have been performed. Here we can track the major differences between UPd_2Ga_3 and UPd_2Al_3 arising from (a) chemical pressure and (b) the superstructure, and their effect on the characteristic electronic parameters (T_N, T_c, γ, CEF, μ_{ord}).

In addition, the alloying experiments yield important information regarding the competition between magnetic exchange and the Kondo effect. The question is in how far a simple concept like the Doniach model[5] can be employed to describe the behavior of U compounds. Previously, it has been shown that the Doniach model qualitatively accounts for the magnetic properties of the 122 compounds.[6] The circumstances allowing the use of the Doniach model seem to arise from the crystallographic and magnetic structure. The 122 compounds crystallize in tetragonal structures and the kind of magnetic ordering appearing in these systems is of the Ising type (AF-I structure). Effectively, this situation creates a strong uniaxial anisotropy, which mimics the one dimensionality of the Doniach model.

In the 123 metals the crystallographic and magnetic anisotropies cannot simply be projected onto a quasi-one-dimensional picture, and a similar description of the physics based solely on the Doniach model does not properly account for the observed properties. Accordingly, Mentink *et al.*[7] proposed a model that still relies on the basic Doniach picture, but is more elaborate by introducing two different interactions governing the RKKY exchange and the Kondo effect.

In this paper we report our bulk measurements on the alloying series $UPd_2(Al_{1-x}Ga_x)_3$. In Sec. II we present the metallurgical analysis of the compounds, and in Sec. III the normal-state resistivity, specific heat, and susceptibility will be described. The evolution of magnetism with alloying is interpreted in terms of the competition between magnetism and the Kondo effect, incorporating the effect of Ga alloying on the CEF splitting. In Sec. IV the superconducting properties of $UPd_2(Al_{1-x}Ga_x)_3$ will be addressed. As a major result we find a complete suppression of superconductivity for small amounts of Ga alloying, contrasting the ineffectiveness of such Ga alloying on the magnetic properties. This observation we take as indication that UPd_2Al_3 is an unconventional superconductor, with a pairing mechanism based presumably on spin fluctuations.

II. METALLURGY

All samples are polycrystals, formed by arc-melting the constituents (purity at least 99.9%) in stoichiometric ratio on

TABLE I. Sample composition (normalized to U=1), amount of second phases, lattice parameters and volume of the unit cells of $UPd_2(Al_{1-x}Ga_x)_3$.

Composition	x	% second	a [Å]	c [Å]
$UPd_{1.84}Al_{2.84}$	0	5	5.368(2)	4.188(2)
$UPd_{1.87}Al_{2.70}Ga_{0.05}$	0.01	1	5.362(2)	4.186(2)
$UPd_{1.85}Al_{2.60}Ga_{0.12}$	0.02	1	5.362(5)	4.184(5)
$UPd_{1.87}Al_{2.73}Ga_{0.20}$	0.05	1	5.356(4)	4.185(5)
$UPd_{1.98}Al_{2.57}Ga_{0.29}$	0.1	5	5.353(4)	4.188(3)
$UPd_{1.97}Al_{2.46}Ga_{0.41}$	0.15	3	5.347(5)	4.187(4)
$UPd_{1.97}Al_{2.27}Ga_{0.55}$	0.2	5	5.344(4)	4.187(4)
$UPd_{2.02}Al_{1.93}Ga_{0.93}$	0.33	5	5.336(5)	4.196(5)
$UPd_{2.00}Al_{0.92}Ga_{1.91}$	0.66	5	5.322(6)	4.212(6)
$UPd_{2.03}Al_{0.44}Ga_{2.41}$	0.8	11	5.323(4)	4.227(5)
$UPd_{2.02}Al_{0.23}Ga_{2.63}$	0.9	13	5.303(3)	8.469(8)
$UPd_2Ga_{2.88}$	1	5	5.3015(1)	8.5112(3)

a water-cooled copper crucible. Subsequently, they have been annealed in high vacuum in quartz ampoules at 900 °C for 1 week. The weight losses of the samples have been monitored after melting and annealing, and were found to be negligible. All materials were checked by electron probe microanalysis (EPMA) and x-ray diffraction for composition and crystallographic structure.

The analysis of $UPd_2(Al_{1-x}Ga_x)_3$, $0 \leqslant x \leqslant 1$, indicated good homogeneity (as evinced by the small percentage of second phase; see Table I) for $x \leqslant 0.66$ and slightly less homogeneity for $x = 0.8$ and 0.9. (The latter samples were considered to be sufficiently pure for the purposes of our comparative study.) The compositions of the matrices, measured by EPMA, are also listed in Table I. The total of Ga plus Al concentration adds up to about 2.8–2.9 instead of 3, probably indicating preferential Ga/Al evaporation during melting.

The lattice parameters and unit-cell volumes of the compounds are included in Table I. The $PrNi_2Al_3$ structure was found for compositions $x \leqslant 0.8$. However, $UPd_2Al_{0.3}Ga_{2.7}$ ($x = 0.9$) forms in the BaB_2Pt_3 superstructure, implying that the crystallographic transition from the $PrNi_2Al_3$ to the BaB_2Pt_3 lattice occurs between $x = 0.8$ and 0.9. In Fig. 1

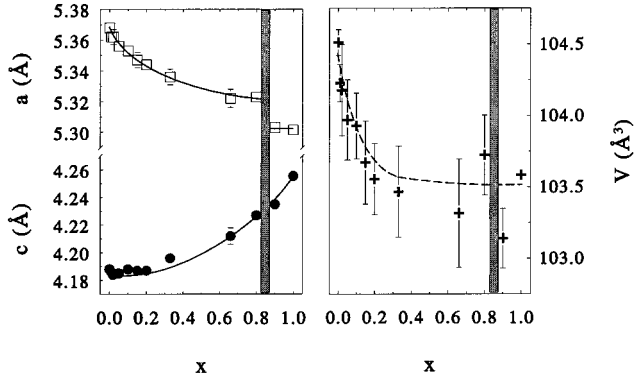

FIG. 1. The lattice parameters a (□) and c (●), and the volume of the unit cell V (+) of $UPd_2(Al_{1-x}Ga_x)_3$ vs Ga concentration x. The shaded bars between $x = 0.8$ and 0.9 mark the structural transition. The lines are guides to the eye.

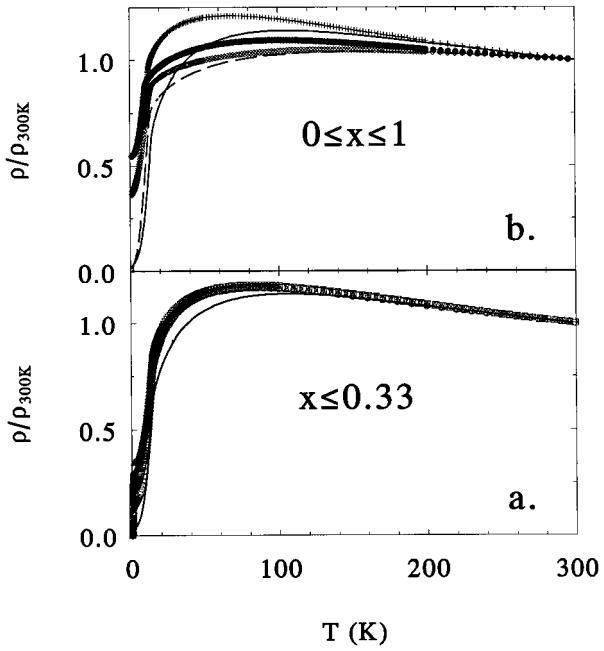

FIG. 2. (a) The normalized resistivity of $UPd_2(Al_{1-x}Ga_x)_3$ for $x = 0$ (–), 0.05 (○), 0.1 (▽), 0.2 (□), and 0.33 (△). (b) As for (a), but now for $x = 0$ (–), 0.66 (+), 0.8 (●), 0.9 (◇), and 1 (– –).

the a and c axis parameters are plotted against Ga concentration x (for $x = 0.9$ and 1, one-half the c axis values are given). Initially, for low Ga concentrations, the a axis decreases linearly, but pronounced deviations from linearity are found at the transition from the $PrNi_2Al_3$ to the BaB_2Pt_3 structure. In contrast, the c axis shows hardly any increase for $x \leqslant 0.2$, while it rises rapidly for larger x without a distinct anomaly at the structural transition. The overall effect of the complete Ga substitution on the unit-cell volume is equivalent to an applied pressure of about 10 kbar.[3]

III. MAGNETISM IN $UPd_2(Al_{1-x}Ga_x)_3$

In Fig. 2 the overall normalized resistivities for $UPd_2(Al_{1-x}Ga_x)_3$ are displayed. All samples $UPd_2(Al_{1-x}Ga_x)_3$ were quite brittle, and we could not determine absolute resistivity values with high accuracy. However, for $x \leqslant 0.33$ there is little difference in the normalized resistivities between 100 and 300 K, implying that $\rho_{300\,K}$ is similar for all samples in this alloying range (about 180 $\pm 10\ \mu\Omega$ cm). For higher Ga concentrations this overlap does not occur and we can only estimate $\rho_{300\,K}$ to about 200 $\pm 50\ \mu\Omega$ cm.

Since for $x \leqslant 0.33$ the normalized resistivities are virtually indistinguishable above 100 K [Fig. 2(a)], the physical mechanism governing the resistivity is not altered for low amounts of Ga substitution. Only below 100 K do the curves for different x begin to deviate from each other mainly due to the collapse of lattice periodicity. The degree of lattice disorder is, to first approximation, measured by the residual resistivity ratio $RRR = \rho_{300\,K}/\rho_{2\,K}$, which is strongly suppressed with increasing x. The magnetic transition temperature, in contrast, is barely affected by Ga alloying. In Fig.

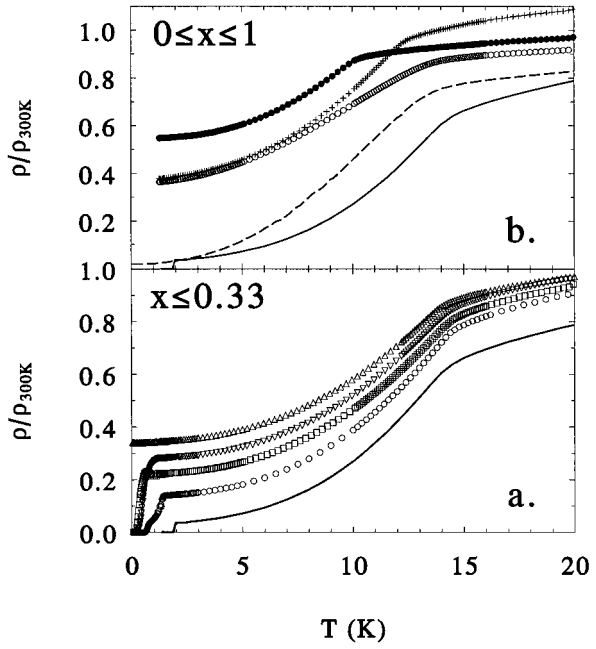

FIG. 3. (a) The antiferromagnetic transition in the normalized resistivity of $UPd_2(Al_{1-x}Ga_x)_3$ for $x = 0$ (–), 0.05 (○), 0.1 (▽), 0.2 (□), and 0.33 (△). (b) As for (a), but now for $x = 0$ (–), 0.66 (+), 0.8 (●), 0.9 (◇), and 1 (– –).

3(a) the low-T region of the normalized resistivity is enlarged for all samples with $x \leqslant 0.33$. The transition temperatures T_N (determined as minimum in $d^2\rho/dT^2$) are about 14.1 – 14.5 K (see Table II).

A different situation is encountered as the Ga concentration is increased above $x \approx 0.33$, as shown in Figs. 2(b) and 3(b) (the values of T_N and RRR are included in Table II). Here the general shape of the curves and T_N shows a pronounced dependence on x. The changing shapes of the curves imply that the CEF splitting shifts with alloying from that of UPd_2Al_3 to UPd_2Ga_3. Further, using the RRR as a measure for disorder, it is reasonable that pure UPd_2Ga_3 exhibits a much larger RRR than the alloyed samples. The most remarkable result, however, is an anomaly in the T_N vs x dependence. We find a jumplike increase of T_N at the structural transition between $x = 0.8$ and 0.9. This implies that the crystallographic superstructure directly affects the magnetic exchange in UPd_2Ga_3.

TABLE II. Antiferromagnetic transition temperatures T_N (derived from normalized resistivity $\rho/\rho_{300\,K}$, specific heat c_p, and susceptibility χ_{dc}), superconducting transition temperatures T_c, the residual resistivity ratio RRR = $\rho_{300\,K}/\rho_{2\,K}$, and the electronic specific heat coefficient γ for $UPd_2(Al_{1-x}Ga_x)_3$.

x	$T_{N;\rho}$ (K)	$T_{N;c_p}$ (K)	$T_{N;\chi}$ (K)	T_c (K)	RRR	γ (J/mole K^2)
0	14.3	14.3	13.8	1.89	28	0.148(5)
0.01	14.5	—	—	1.64	18	–
0.02	14.5	—	13.9	1.51	9.4	–
0.05	14.5	—	13.9	1.15	7.0	–
0.1	14.5	14.3	13.7	0.52	3.5	0.149(5)
0.15	14.5	—	13.5	0.76	4.0	–
0.2	14.4	14.0	13.6	0.33	4.4	0.144(5)
0.33	14.1	13.2	13.2	< 0.05	2.9	0.147(5)
0.66	12.3	11.6	11.5	< 0.05	2.6	0.184(5)
0.8	10.2	9.7	9.46	< 0.05	1.8	0.191(5)
0.9	13.5	12.8	12.0	< 0.05	2.7	0.226(5)
1	13.1	13	12.2	< 0.05	30	0.230(5)

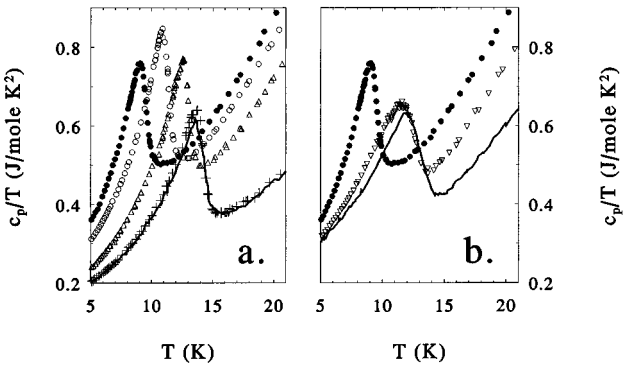

FIG. 4. (a) The specific heat divided by temperature c_p/T vs temperature T of $UPd_2(Al_{1-x}Ga_x)_3$ with $x = 0$ (–), 0.1 (+), 0.33 (△), 0.66 (○), and 0.8 (●), and (b) with $x = 0.8$ (●), 0.9 (▽), and 1 (–).

In addition, we studied the antiferromagnetic transitions of $UPd_2(Al_{1-x}Ga_x)_3$ by specific heat (depicted as c_p/T against T in Fig. 4). The peaks of the transition are clearly visible; the transition temperatures T_N, determined by entropy balance, are included in Table II. Although these are slightly lower than those obtained from the resistivity, the major feature, the jump of T_N at the structural transition, reproduces well.

For $x \leqslant 0.2$ little effect of the Ga substitution is resolvable in the specific heat, if compared to UPd_2Al_3 [Fig. 4(a)]. Further, the shape of the antiferromagnetic transition is not strongly altered with the replacement of Al by Ga for $x \leqslant 0.8$, but it suddenly broadens after the structural transition [Fig. 4(b)]. Also, the absolute values of c_p above T_N go through a maximum at the structural transition. Both effects can partially be attributed to a shift of the energy splitting of the low-lying CEF levels with Ga alloying. We have already described the dependence of the shape of the magnetic transition in c_p on the particular CEF level scheme in Ref. 8. Further, the maximum of the absolute c_p values above T_N for $x = 0.8$ indicates that the CEF energy splitting does not change linearly with Ga substitution, but that there is an anomaly of the level splitting at the transition from the $PrNi_2Al_3$ to the BaB_2Pt_3 lattice (with the introduction of the superstructure the electric field gradients at the U site, and thus the CEF scheme, will be affected). In addition to this CEF shift with x, there is also an effect of the Ga alloying on the phonon spectrum. At present, we cannot assess from the specific heat the full extent of the changes in the CEF scheme or the phonon spectrum and are unable to quantify these modifications.

For all samples c_p/T is linear in T^2 below the magnetic transition regime at T_N, and therefore, we can derive the electronic specific heat γ as function of x. The values of γ for $UPd_2(Al_{1-x}Ga_x)_3$ (extrapolated between 2 and 10 K for $x = 0$ and 1, 4.5, and 10 K for $0 < x < 0.8$ and $x = 0.9$, and

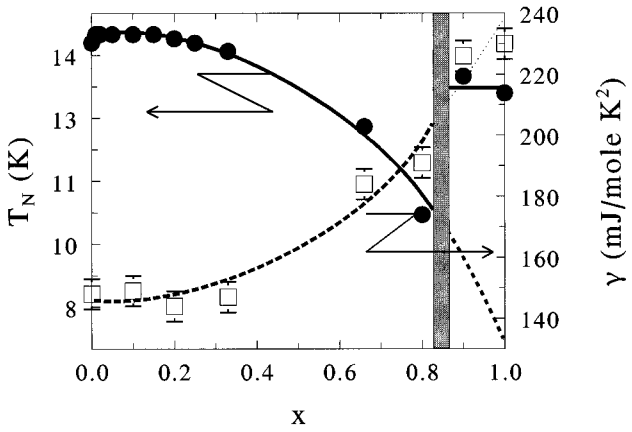

FIG. 5. The antiferromagnetic phase diagram (●) for $UPd_2(Al_{1-x}Ga_x)_3$ (from the resistivity) and the electronic contribution to the specific heat γ (□).

4.5 and 8 K for $x = 0.8$) are included in Table II and plotted in Fig. 5. The plot illustrates the evolution of T_N (derived from $\rho/\rho_{300\,K}$) and γ with x for $UPd_2(Al_{1-x}Ga_x)_3$. The shaded region in the diagram denotes the structural transition regime. From the figure it is obvious that γ does not scale with T_N over the whole alloying range. We will reconsider this feature in the discussion.

Finally, we measured the susceptibility of $UPd_2(Al_{1-x}Ga_x)_3$ (Fig. 6). The antiferromagnetic transition temperatures (determined from the maximum in $d(\chi T)/dT$) are included in Table II and exhibit, as the specific heat and the resistivity, an anomaly of T_N between $x = 0.8$ and 0.9. Also, we find a close connection between the shape of χ and the Ga alloying. For $x \leqslant 0.2$ little change in the shape of χ is seen (not shown). Then, for $0.33 \leqslant x \leqslant 0.8$, the height of the maximum in χ increases, the maximum shifts to lower temperatures, and its shape is preserved. Suddenly, at the structural transition, the shape is altered as well, and the CEF maximum coincides with the antiferromagnetic transition.

The dependence of χ can be understood in terms of the CEF splitting. In order to illustrate this, we apply the CEF model, used to simulate c_p of UPd_2Ga_3 in Ref. 8, and calculate the susceptibility. The results are shown in Fig. 7, and they give a general impression of the dependence of χ on the CEF splitting for UPd_2Ga_3, UPd_2Al_3, and the intermediate case of $UPd_2(Al_{0.2}Ga_{0.8})_3$. The CEF splitting consists of a singlet ground state Δ_0 and an excited singlet Δ_1, mixing with a doublet Δ_2 at higher temperatures.[9] The energy splittings are given in the plot.

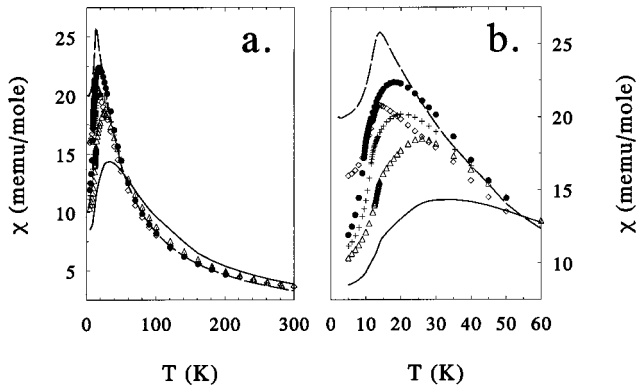

FIG. 6. The susceptibility χ below 300 K (a) and 60 K (b) of $UPd_2(Al_{1-x}Ga_x)_3$ with $x = 0$ (–), 0.33 (△), 0.66 (+), 0.8 (●), 0.9 (◇), and 1 (– –).

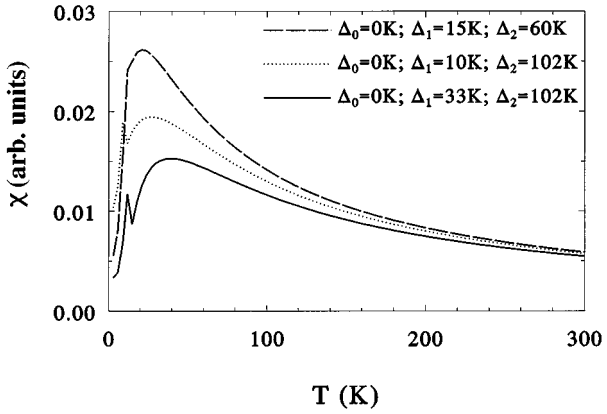

FIG. 7. A molecular field simulation of the susceptibility of $UPd_2(Al_{1-x}Ga_x)_3$ according to the CEF scheme described in the text, with the splitting energies given in the plot. The three calculations correspond to the cases of UPd_2Al_3 (–), UPd_2Ga_3 (– –), and $UPd_2(Al_{0.2}Ga_{0.8})_3$ (· · ·).

As with all simple mean-field models, there are deficiencies. No short-range order fluctuations at T_N have been introduced, and we find the calculated antiferromagnetic peaks not fully matching the experimental observations. Moreover, the heavy-fermion Pauli paramagnetism and the high-lying CEF levels are disregarded. Still, the model reproduces the main features of the experiment. From the calculation the general trend of alloying from UPd_2Al_3 to UPd_2Ga_3 is to shift the CEF maximum below the magnetic transition of UPd_2Ga_3. The ratio of maxima for different x is properly described. Finally, the anomalous CEF behavior at the structural transition seems to indicate that with Ga alloying for $x \leqslant 0.8$ (in the $PrNi_2Al_3$ structure) the splitting between the ground state Δ_0 and the excited singlet Δ_1 diminishes. After the structural transition the splitting between Δ_0 and the doublet Δ_2 decreases, while Δ_1 increases slightly.

We now return to the phase diagram shown in Fig. 5. Obviously, T_N and γ scale as long as the $PrNi_2Al_3$ structure is preserved. The decrease of T_N, signifying a weakening of magnetism and a reduction of the ordered magnetic moment, is accompanied by the increase of γ. However, at the structural transition T_N exhibits a jumplike increase, indicating that the magnetic exchange is strengthened. In contrast, we do not find a similar anomaly in γ, which instead increases (possibly with a small upward jump) through the structural transition. Apparently, the hybridization is not strongly dependent on the U local site symmetry.

This finding implies that a description of the alloy system $UPd_2(Al_{1-x}Ga_x)_3$ entirely in terms of the Doniach model fails. The structural changes in the system, which heavily affect the magnetism, cannot be accounted for in this model. Only as long as the $PrNi_2Al_3$ structure is kept can the scaling between γ and T_N be qualitatively described within a Doniach-like picture. In our opinion the evolution of magne-

tism in $UPd_2(Al_{1-x}Ga_x)_3$ can be elucidated in a phenomenological model as follows.

(a) The hybridization exchange $J_{f\text{-}s,p,d}$ depends mainly on the unit-cell volume. It is not (or only weakly) dependent on the details of the crystallographic structure, but primarily related to the distance between the magnetic and metallic atoms. Its value is determined by the volume of the unit cell and the average overlap of the U-metal orbitals. In the Doniach picture a hybridization energy scale is set by $J_{f\text{-}s,p,d}$ according to[5]

$$E_{f\text{-}s,p,d} \sim \frac{\exp\{-1/[N(0)J_{f\text{-}s,p,d}]\}}{N(0)}. \tag{1}$$

(b) Because of the simplicity of the magnetic structure in $UPd_2(Al_{1-x}Ga_x)_3$, viz., the antiferromagnetic arrangement along the c axis of spins ferromagnetically coupled in the hexagonal basal plane, we can omit from further consideration the magnetic exchange in the hexagonal plane. Here the coupling is always ferromagnetic, as it is stabilized either through strong internal fields or simply by the hexagonal symmetry. This avoids problems with frustration or complex magnetic structures in the basal plane which could occur if the interactions were antiferromagnetic.[10,11] The crucial magnetic exchange along the c axis seems to be well described by a usual RKKY oscillatory type of interaction $J_{\mathrm{RKKY}}(c)$. Its energy scale is set in the Doniach representation by

$$E_{\mathrm{RKKY}} \sim N(0)J^2_{\mathrm{RKKY}}(c). \tag{2}$$

Our model closely resembles the one proposed by Mentink *et al.*,[7] only we have removed the assumption of an anisotropic hybridization $J_{f\text{-}s,p,d}$.

Accordingly we can describe the observed evolution of the magnetic properties in $UPd_2(Al_{1-x}Ga_x)_3$: When alloying UPd_2Al_3 with Ga, the volume of the unit cell and the U-Pd distance (as leading term of the hybridization strength) decrease, and, correspondingly, $J_{f\text{-}s,p,d}$ and γ increase. $J_{\mathrm{RKKY}}(c)$ (as long as the $PrNi_2Al_3$ structure is retained) decreases with the increasing c axis. Both effects work in concord and T_N is reduced.

At the structural transition the RKKY exchange is strongly affected and T_N increases discontinuously. In contrast, γ hardly exhibits any anomaly, since the average U-metal distances as well as the volume of the unit cell change smoothly through the structural transition. (As mentioned above, there might be a small jumplike increase of γ at the transition; nevertheless, it does not affect our argument, as both γ and T_N increase, indicating the breakdown of scaling.) Proof that mainly $J_{\mathrm{RKKY}}(c)$ changes discontinuously at the transition is the hypothetical value of T_N for superstructure-free UPd_2Ga_3. As noted in Ref. 3, there is a discrepancy between the decrease of μ_{ord} and T_N with full replacement of Al by Ga in UPd_2Al_3. While μ_{ord} is 1.7 times smaller in UPd_2Ga_3 than in UPd_2Al_3, T_N is lowered only by a factor 1.1. However, as is illustrated by the extrapolation of T_N to $x = 1$, indicated in Fig. 5, the hypothetical value of T_N for UPd_2Ga_3, crystallizing in the $PrNi_2Al_3$ structure, would be about 7 K. This reduction of T_N would be in much better agreement with the reduction of μ_{ord} and the increase of γ.

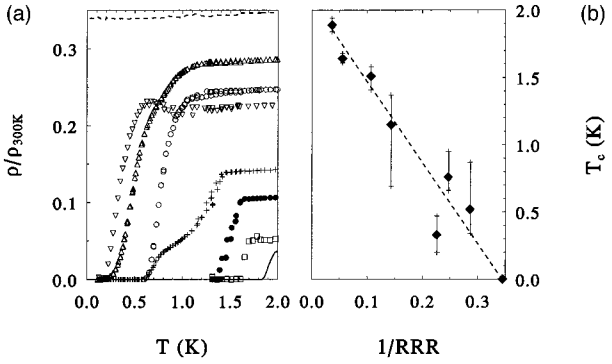

FIG. 8. (a) The superconducting transitions of $UPd_2(Al_{1-x}Ga_x)_3$: $x = 0$ (–), 0.01 (□), 0.02 (●), 0.05 (+), 0.1 (△), 0.15 (○), 0.2 (▽), and 0.33 (– –). (b) The relation between T_c and the residual resistance ratio RRR. Bars indicate 10% and 90% points of the transitions.

IV. SUPERCONDUCTIVITY IN $UPd_2(Al_{1-x}Ga_x)_3$

For small amounts of Ga the specimens of $UPd_2(Al_{1-x}Ga_x)_3$ still exhibit superconductivity. The superconducting transition temperatures are determined by resistivity measurements; the transition curves are depicted in Fig. 8(a). The transition temperatures (determined as the 50% point of the resistance drop) are included in Table II.

Several of the curves show broad and double transitions indicating metallurgical imperfections. In order to check if secondary phase superconductivity is the source of the transition broadening we compared the Meissner effect for several samples. These measurements indeed show that samples with $x > 0.1$ are not bulk superconductors, since they exhibit Meissner fractions only of about 10–20 %. For lower Ga concentrations, however, the samples are indeed bulk superconductors.

This finding implies that another experimental feature has to be taken with caution. From the resistance data it might be concluded that T_c scales with the RRR. In Fig. 8(b) this is illustrated by plotting T_c against RRR. In fact, such dependence has been claimed before, based on alloying experiments on UPd_2Al_3 with a large group of dopants.[12] Remarkably, the correlation between T_c and RRR even holds reasonably well for $UPd_2(Al_{1-x}Ga_x)_3$ with $x > 0.1$, thus for nonbulk superconducting samples. Hence, for larger quantities of Ga substitution (and for other dopants?) the correlation between T_c and RRR is fortuitous. Still, for low Ga amounts there exists a relation between the reduction of the RRR (being a measure of the mean free path in this Ga alloying range) and T_c. A similar relationship between mean free path and reduction of T_c had been found for another heavy-fermion superconductor, UPt_3.[13]

We argue that the strong suppression of T_c and the mean free path with Ga doping indicates unconventional superconductivity in UPd_2Al_3. This interpretation of the alloying experiments on $UPd_2(Al_{1-x}Ga_x)_3$ is based on the superconducting and magnetic phase diagrams (Fig. 9). While the magnetic behavior is unaffected by Ga alloying up to $x \approx 0.3$, superconductivity fully vanishes at $x = 0.25$. This indicates that the nonmagnetic Ga acts as an effective pair breaker (we ignore the problem of the broad superconducting transitions, since it does not affect the primary result of the

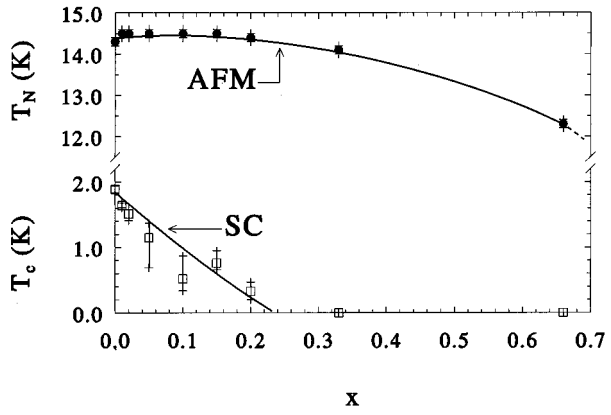

FIG. 9. Antiferromagnetic and superconducting phase diagrams of $UPd_2(Al_{1-x}Ga_x)_3$. T_N and T_c are both determined via resistance measurements.

complete suppression of superconductivity by Ga doping). Now, according to several authors, for unconventional superconductivity, the pair-breaking effect due to nonmagnetic impurities could be of the same order as that observed for magnetic ones in conventional superconductors.[14–16] In particular, Millis *et al.*[16] pointed out that a T_c depression in unconventional superconductors by nonmagnetic pair breakers is coupled to the reduction of the mean free path of the electrons. Since up to an alloying rate of $x \leqslant 0.33$, apart from the RRR reduction, virtually no changes appear in the normal-state properties of $UPd_2(Al_{1-x}Ga_x)_3$—T_N, γ, and the CEF splitting remain essentially constant—we can safely assume that other pair-breaking mechanisms (for instance, magnetic ones) are not affected by the Ga alloying. Only the nonmagnetic pair breaking by the Ga can cause the dramatic suppression of T_c.

There is further evidence that this scenario applies to UPd_2Al_3. Millis *et al.*[16] investigated the pair-breaking effect of spin fluctuations in a *d*-wave superconductor and found that low-frequency spin fluctuations act as effective pair breakers, while the high-frequency spin fluctuations tend to be pair forming. A change in the spin fluctuation spectrum of a *d*-wave superconductor should therefore be reflected in T_c. From bulk data it is difficult to obtain accurate information on the spin fluctuation spectrum of a particular compound. Some insight can be gained from the low-temperature magnetic resistivity. For two similar magnetic compounds (like UPd_2Al_3 and UPd_2Ga_3) the T^2-coefficient of the resistivity A reflects the spin fluctuations: The larger the value of A, the lower the average spin fluctuation frequency. Thus, in our case, the nonsuperconducting UPd_2Ga_3 should have a much larger value of A than UPd_2Al_3, in agreement with experiment. While in UPd_2Ga_3 a value $A = 0.66$ $\mu\Omega$ cm/K^2 is reported,[3] for UPd_2Al_3 a significantly smaller value $A = 0.26$ $\mu\Omega$ cm/K^2 is found.[17]

Finally, recent NMR and NQR measurements on UPd_2Ga_3 and UPd_2Al_3 (Refs. 18–20) indicate pronounced differences in the spin fluctuation spectra of the two compounds. Unfortunately, from these measurements it could not be unambiguously concluded whether the average spin fluctuation frequency is higher in UPd_2Al_3 or UPd_2Ga_3. Further experiments and analysis are underway to clarify this point.

V. CONCLUSIONS

Summarizing our results on $UPd_2(Al_{1-x}Ga_x)_3$ leads to the following conclusions.

(a) The magnetic properties of UPd_2Al_3, UPd_2Ga_3, and the intermediate quasiternary compounds are qualitatively similar. The small quantitative differences can be understood if the influence of the crystallographic superstructure on the RKKY exchange along the *c* axis is taken into account. As long as the $PrNi_2Al_3$ structure is preserved, the physical quantities γ, T_N, and $\mu_{\rm ord}$ scale with the Ga concentration. This scaling can be understood in a model utilizing the *c* axis RKKY exchange $J_{\rm RKKY}$ and the volume hybridization $J_{f\text{-}s,p,d}$. At the structural transition $J_{\rm RKKY}$ is strongly affected, while $J_{f\text{-}s,p,d}$ is not, leading to a breakdown of the scaling.

(b) The remarkable pair-breaking effect of nonmagnetic Ga is a strong indication for unconventional superconductivity. Here the absence of superconductivity in UPd_2Ga_3 would be attributed to differences in the spin fluctuation spectrum between UPd_2Ga_3 and UPd_2Al_3, which is qualitatively in agreement with experimental findings. Nevertheless, the final proof for unconventional superconductivity in UPd_2Al_3, namely, a quantitative comparison of the spin fluctuation spectra of UPd_2Al_3 and UPd_2Ga_3, is still lacking.

ACKNOWLEDGMENTS

We gratefully acknowledge the experimental assistance of S. Ramakrishnan and C. C. Mattheus as well as fruitful discussions with S.A.M. Mentink. The samples have been made by FOM-ALMOS. Part of this research was performed under the auspices of the Nederlandse Stichting voor Fundamenteel Onderzoek der Materie (FOM).

[1] C. Geibel, S. Thies, D. Kaczorowski, A. Mehner, A. Grauel, B. Seidel, U. Ahlheim, R. Helfrich, K. Petersen, C. D. Bredl, and F. Steglich, Z. Phys. B **83**, 305 (1991).

[2] C. Geibel, C. Schank, S. Thies, H. Kitazawa, C. D. Bredl, A. Böhm, M. Rau, A. Grauel, R. Caspary, R. Helfrich, U. Ahlheim, G. Weber, and F. Steglich, Z. Phys. B **84**, 1 (1991).

[3] S. Süllow, B. Ludoph, B. Becker, G. J. Nieuwenhuys, A. A. Menovsky, J. A. Mydosh, S. A. M. Mentink, and T. E. Mason, Phys. Rev. B **52**, 12 784 (1995).

[4] R. H. Heffner and M. R. Norman, Comments Condens. Matter Phys. **17**, 361 (1996).

[5] S. Doniach, in *Valence Instabilities and Related Narrow-Band Phenomena*, edited by R. D. Parks (Plenum, New York, 1977), p. 169; Physica B **91**, 231 (1977).

[6] T. Endstra, G. J. Nieuwenhuys, and J. A. Mydosh, Phys. Rev. B **48**, 9585 (1993).
[7] S. A. M. Mentink, G. J. Nieuwenhuys, A. A. Menovsky, J. A. Mydosh, H. Tou, and Y. Kitaoka, Phys. Rev. B **49**, 15 759 (1994).
[8] S. Süllow, B. Ludoph, G. J. Nieuwenhuys, A. A. Menovsky, and J. A. Mydosh, Physica B **223&224**, 208 (1996).
[9] A. Grauel, A. Böhm, H. Fischer, C. Geibel, R. Köhler, R. Modler, C. Schank, F. Steglich, G. Weber, T. Komatsubara, and N. Sato, Phys. Rev. B **46**, 5818 (1992).
[10] S. Teitel and C. Jayaprakash, Phys. Rev. B **27**, 598 (1983).
[11] D. H. Lee, J. D. Joannopoulos, J. W. Negele, and D. P. Landau, Phys. Rev. Lett. **52**, 433 (1984).
[12] C. Geibel, C. Schank, F. Jährling, B. Buschinger, A. Grauel, T. Lühmann, P. Gegenwart, R. Helfrich, P. H. P. Reinders, and F. Steglich, Physica B **199&200**, 128 (1994).
[13] Y. Dalichaouch, M. C. de Andrade, D. A. Gajewski, R. Chau, P. Visani, and M. B. Maple, Phys. Rev. Lett. **75**, 3938 (1995).
[14] R. Balian and R. Werthamer, Phys. Rev. **131**, 1553 (1963).
[15] P. Hirschfeld, D. Vollhardt, and P. Wölfle, Solid State Commun. **59**, 111 (1986).
[16] A. J. Millis, S. Sachdev, and C. M. Varma, Phys. Rev. B **37**, 4975 (1988).
[17] R. Caspary, P. Hellmann, M. Keller, G. Sparn, C. Wassilew, R. Köhler, C. Geibel, C. Schank, F. Steglich, and N. E. Phillips, Phys. Rev. Lett. **71**, 2146 (1993).
[18] H. Tou, Y. Kitaoka, T. Kamatsuka, K. Asayama, C. Geibel, F. Steglich, S. Süllow, and J. A. Mydosh, Physica B **230-232**, 360 (1997).
[19] M. Kyogaku, Y. Kitaoka, K. Asayama, C. Geibel, C. Schank, and F. Steglich, J. Phys. Soc. Jpn. **62**, 4016 (1993).
[20] H. Tou, Y. Kitaoka, K. Asayama, C. Geibel, C. Schank, and F. Steglich, J. Phys. Soc. Jpn. **64**, 725 (1995).